IAHR AIRH

SYMPOSIUM 1990

BELGRADE YUGOSLAVIA

H3

VIBRATORY CHARACTERISTICS OF EROSIVE CAVITATION VORTICES DOWNSTREAM OF A FIXED LEADING EDGE CAVITY

Caractéristiques vibratoires de l'érosion génerée par des cavités tourbillonaires à l'aval d'une cavitation de bord d'attaque

Bourdon, Paul	Eng.	Hydro Québec	Canada
Simoneau, Raynald	Ph.D.	Hydro Québec	Canada
Avellan, François	Ph.D.	IMHEF-EPFL	Switzerland
Farhat, Mohamed	Eng.	IMHEF-EPFL	Switzerland

ABSTRACT

To identify the distinctive vibratory characteristics of erosive cavitation an investigation program was conducted in the IMHEF High Speed Cavitation Tunnel on a NACA 009 stainless steel profile equipped with 7 DECER electrochemical cavitation erosion detectors and high frequency vibration sensors. Forces acting on the profile were inferred from a measured transmissibility function.Above a low threshold value a linear relationship was found between the measured mean square value of acceleration and the average erosion rate on the profile. Erosion vortices were found to be shed away from the main leading edge cavity according to a constant Strouhal number law. Their hydrodynamic erosive intensity of a power dimension, proportional to $V^{3}l^{2}$, is defined. This intensity is linearly related to the measured RMS force and average erosion on the profile for a given set of incidence and sigma values. The erosive efficiency of the cavitating flow however decreases with σ.

RESUME

Une campagne de mesures a été menée sur un profil bidimensionnel NACA 009 en acier inoxydable muni de 7 sondes électrochimiques DECER de détection de cavitation érosive et de capteurs de vibration haute fréquence. À l'aide d'une fonction de transmissibilité mesurée, les forces dynamiques agissant sur le profil ont été inferées. Une relation linéaire lie la valeur quadratique moyenne de l'accélération et le taux d'érosion moyen . Les vortex érosifs sont générés par une poche de cavitation de bord d'attaque suivant une fréquence de Strouhal constante. Une intensité hydrodynamique d'érosion homogène à une puissance et proportionnel à $V^{3}l^{2}$, a été établie. Cette intensité est reliée de manière linéaire à l'érosion moyenne et à la valeur quadratique moyenne des forces mesurées sur le profil pour une combinaison de valeurs d'incidence et de sigma. De plus, l'efficacité érosive de l'écoulement cavitant diminue avec le chiffre de cavitation.

NOMENCLATURE

L	=	Chord length	[m],	l	=	cavity length	[m]
p_0	=	Upstream static pressure	[Pa]	V	=	Upstream velocity	[m·s^{-1}]
p_v	=	Vapor pressure	[Pa]	ρ	=	Water density	[kg·m^{-3}]
p_{max}	=	cavity closure back pressure	[Pa]	p	=	Static pressure	[Pa]
C_p	=	Pressure coefficient	[-]	σ	=	Cavitation number	[-]
E	=	cavitation potential energy	[J]	$\dot{E}$	=	mean erosive power	[W]

INTRODUCTION.

The identification of the presence and intensity of erosive cavitation on operating hydraulic machines remains of interest to their operators and designers. In order to achieve this objective, the distinctive characteristics of erosive cavitation must be identified. Systematic comparisons between visualizations carried out during model tests and observations of damage on prototype blades have allowed to identify erosive cavities as swirling transient vortices shed away in the closure region of the main leading edge cavity. In this region of the flow where a pressure recovery takes place, the transient vortices are subjected to collapse leading to blade erosion.
Past research efforts by Avellan et al. at IMHEF [1,2] in the High Speed Cavitation Tunnel have supported this explanation and recent investigations [3] by Simoneau et al. have confirmed this point. Direct electrochemical erosion measurements coupled with simultaneous vibration measurements on operating models of Francis turbines by Simoneau and Bourdon [4,5] have shown promising correlations under those conditions where erosion levels could be detected. The vibratory measurement techniques used in the laboratory on the models have also given results on prototypes which are consistent with the cavitation erosion histories of these machines [6].
Having thus at hand an erosion mechanism model, an on-line erosion measurement method and a vibratory cavitation detection technique, it was decided that further investigations would be performed into the vibratory characteristics of erosive cavitation vortices with the hope of calibrating the vibratory technique against measured erosion rates. In particular, it was hoped that acting forces during the erosion attack could be inferred from acceleration measurements on the test NACA profile.

TEST SETUP.

To perform these investigations, a NACA 009 2D stainless steel profile was fabricated with seven DECER electrochemical erosion detectors [3,4,7,8] mounted flush with the suction surface. The blade was mounted in the IMHEF High-Speed Cavitation Tunnel as shown in Figure 1. A miniature high frequency accelerometer with a mounted resonance frequency of 90 kHz and a wideband acoustic emission sensor operating in the 100 to 1000 kHz frequency band were fixed to the blade embedment housing within 30 mm of the blade itself (see Fig.1). The data acquisition systems that were utilized in the experimentation program are illustrated in Figure 2. Stroboscopic photographs of the NACA profile were taken at the beginning and end of each test.

Dynamic characterization of the NACA profile.

In order to infer excitation forces on the profile under cavitating conditions from measured acceleration values, it is necessary to first measure the transmissibility function which is the ratio of

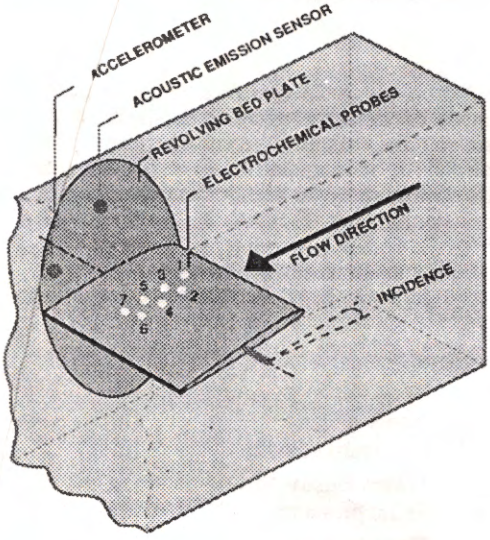

Fig. 1 The probes on the NACA profile.

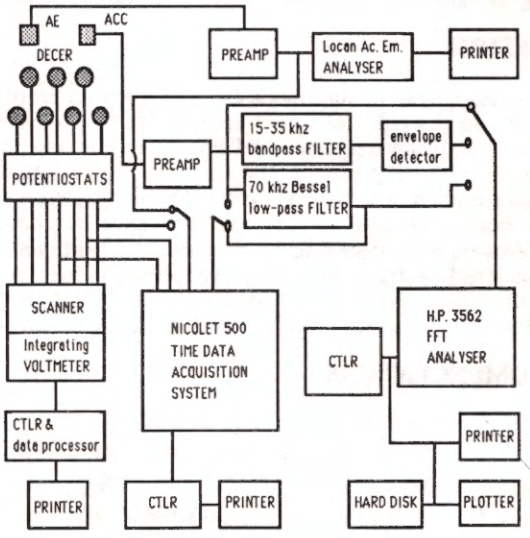

Figure 2 Data acquisition system.

the output acceleration autospectrum to the input force autospectrum. This was realized in the 0-50kHz frequency band by exciting the profile with a miniature instrumented force hammer and measuring the vibration response of the profile almost completely submerged with the accelerometer mounted at the position occupied during all of the subsequent hydraulic tests. An averaged transmissibility function was measured by exciting the profile five times next to DECER probes 1 to 5. The measured transmissibility function appears in Figure 3. To recover the autospectrum of the excitation forces on the profile during cavitation tests it is then only necessary to divide the measured acceleration autospectrum for any given test condition by this transmissibility function. The mean square value of the acting forces in a frequency band can then be obtained by summing the amplitude values at each frequency in that band. With the knowledge of these force values one can then estimate the order of magnitude of impact stresses by considering the impact area (~1 mm^2) of the force hammer used to establish the transmissibility function.

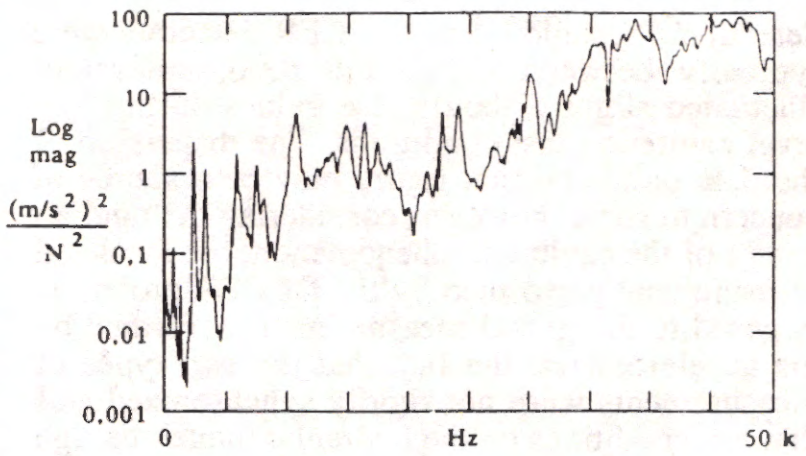

Fig. 3 Acoustic transmissibility function.

EXPERIMENTAL RESULTS.

Erosion vs acceleration

During the test program the cavitation tunnel parameters were varied over the following ranges: blade tilt angle, 2.5 to 4.5 degrees, water velocity, 20 to 42 m/sec, and cavitation number σ, 0.7 to 1.4. We will now present the main results of the experimentation program. We will deal essentially with values derived from acceleration and erosion measurements. Measurements obtained with the higher frequency acoustic emission sensor are consistent with the acceleration signals but due to an apparent saturation phenomena within the sensor itself it was necessary to relocate it further away from the profile for the last two thirds of the tests, making data interpretation more difficult. Results from these latter tests will be presented.

The primary data obtained are shown in Figures 4 and 5. Figure 4 presents the average erosion rate measured over the seven Decer probes for various sets of blade tilt angles, water velocity and cavitation parameter σ. Figure 5 gives the MSV(mean square value) of acceleration measured in the 15 to 35 kHz frequency band for the same operating conditions. All of the data points, including a few which were not plotted in Figures 4 and 5, are plotted on a linear scale in Figure 6 which shows a linear relation between the average erosion rate and the MSV of acceleration.

The least squares linear regression curve fit shown on Fig.6 was based on the data points showing average erosion rates of 0.01mm/a and above. For erosion rates below this value the accuracy of the measurement drops off since the

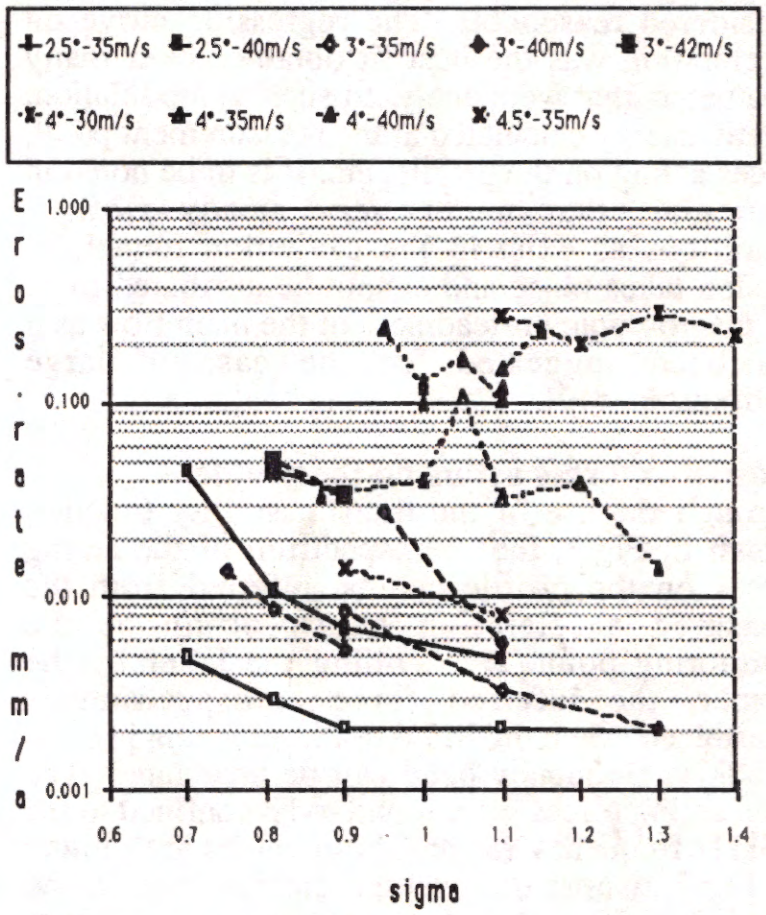

Fig.4 DECER Average erosion rates.

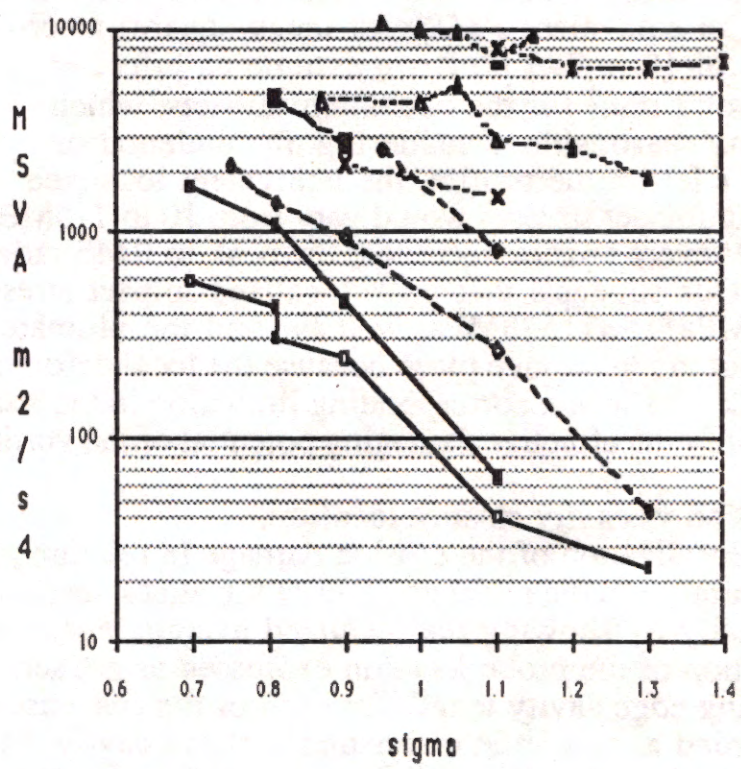

Fig.5 Mean square value of acceleration.

H3

detection threshold on the DECER detectors were typically between 0.001 and 0.005mm/a and fluctuated slightly about these values during low level cavitation test conditions. The dispersion of the data points on that figure may be a source of concern to some; however, considering the random nature of the cavitation phenomenon, the localized measurement performed by the DECER probes as opposed to the global measurement performed by the accelerometer, the fact that the two types of measurements were not rigidly synchronized and that test conditions on the hydraulic tunnel, though very stable on a mean basis, do vary slightly during a test sequence, such a dispersion in results can be considered reasonable. The regression curve on acceleration was the best fit obtained over many parameters that were analyzed such as modulation, kinetic energy calculated at the measurement point, forces acting on the profile, etc. It is to be noted in particular, that under very steady flow conditions as exist in the cavitation tunnel, erosion takes place and cannot be attributed to the macroscopic unsteadiness of the main flow as it has been suggested for the case of large hydroturbines [9].

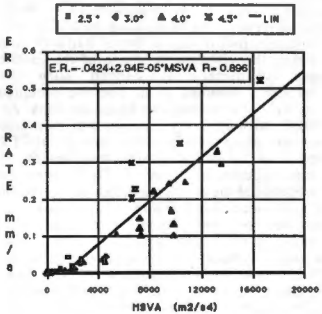

Fig.6 Linear regression erosion vs acceleration.

Erosion vs forces acting on the profile.

Through the use of the transmissibility function shown in Fig.3, the autospectrum of the acting forces on the profile can be inferred from the measured acceleration autospectrum at the monitoring point. By dividing the latter by the former, the inferred force autospectrum is determined. Then the MSV of forces acting in the 0 to 50kHz frequency band can be calculated. The main acting forces were found to be confined to the 0-3kHz frequency range. These values are plotted on Fig.7 against the average erosion rate on the seven DECER probes. It can be seen on that figure that the MSV value of inferred forces spans the range of 100 to 600 000 N^2. This would translate into an equivalent RMS(root mean square) force span of 10 to 775 N. If we assume an effective area of 1 mm^2 for the cavitation impacts, which seems reasonable considering the indentation marks let on the profile, the equivalent localized acting impact stresses would vary from 10 to 775MPa in a RMS sense. Furthermore, in the case of the most severe erosion recorded, the peak to RMS ratio of the response acceleration was observed to be 15. This suggests that peak localized impact stresses under those conditions could be as high as 775MPa*15=11625MPa, well beyond the ultimate strength of the best alloys. Such high stresses cannot in reality take place because the local deformation of the material will cause a stretching of the attack area with a corresponding limitation in the attainable peak stresses. These inferred force values quantify the effective damaging potential of the vortices.

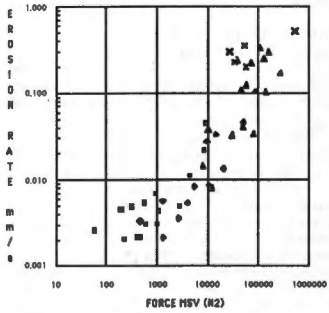

Fig. 7 Erosion vs inferred force on the profile.

Erosion vs cavity closure location.

The localization of the erosion damage in relation to the attached leading edge cavity is of course of importance in the understanding of the attack mechanism. Figure 8 illustrates how erosion takes place spatially by showing the localized average erosion rate on each of the seven DECER probes as a function of the probe location expressed as a fraction of the profile chord length. Also shown is the leading edge cavity length for each of the five cases presented. In all cases the maximum erosion is recorded at or a little downstream of the cavity closure. This again agrees with the damage model derived from model turbine visualizations and actual prototype erosion damage [1] and with the results

H3

of previous tests on the High Speed Cavitation Tunnel [3]. For a constant velocity of 35m/s and blade tilt of 4.5 degrees, the leading edge cavity lengthens when σ decreases from 1.4 to 1.1. The effect of increased velocity to 37m/s for a σ value maintained at 1.4 is to increase slightly the length of the leading edge cavity and to double the localized erosion rate on the second DECER sensor. For that particular sensor under the two sets of test conditions, this increase represents a power of 12 dependance of the erosion on the flow velocity. Essentially though, in this case as in the other four that are illustrated on Fig.8, the highest erosion rates are recorded in the closure area of the leading edge cavity.

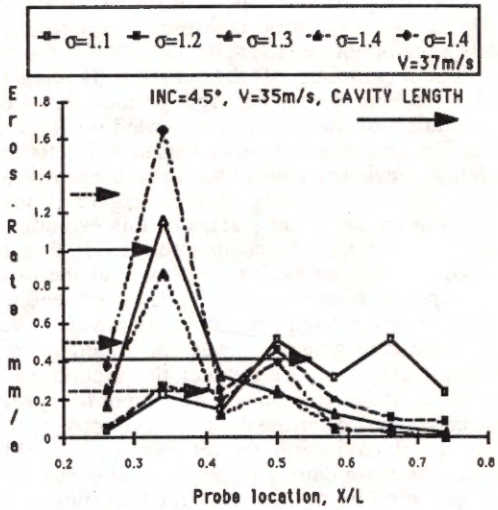

Fig.8 Localization of erosion and cavitation cloud.

Instantaneous erosion vs profile acceleration.

The vibratory approach to the detection of erosive cavitation assumes that under strong erosive conditions the attacked structure is strongly excited mechanically by the imploding cavities [6]. In order to verify this point simultaneous recordings of instantaneous erosion and acceleration signals were made. The test conditions wvortices.

Figure 9 shows four one second time traces recorded simultaneously under those test conditions. The upper trace is the output of the unfiltered accelerometer dominated by its resonance response; this signal was sampled at a 1 MHz rate. All signals in this graph are represented in a min/max mode, that is, the minimum and maximum value of each successive 1000 sample group are plotted one below the other and are joined by a vertical line. This representation illustrates in a condensed graph, the amplitude variation of the envelope of a 10^6 point waveform. The lower three traces from top to bottom represent respectively the outputs of DECER sensors #1, 2 and 4(refer to Fig.1). It is quite clear that sensor #2 located downstream of the cavity closure is suffering from heavy erosion. The erosion as calculated in the data processing equipment is equal to the area under the DECER time curve. When a piece of material on the probe surface is eroded away, a spike in the sensor output occurs and the repassivation of the eroded surface begins. This process which is an electrochemical rebuilding of the probe's oxide layer corresponds to the decaying portion of the trace. The duration of this activity is proportional to the amount of oxide removed initially. If an additional piece of material is eroded before the repassivation is completed, then the trace spikes up again and the overall time for complete repassivation is longer.

All of the erosion spikes are associated with acceleration spikes on the top trace. This is particularly evident for the two major spikes, the one at the beginning and the other at the end of this one second time record.

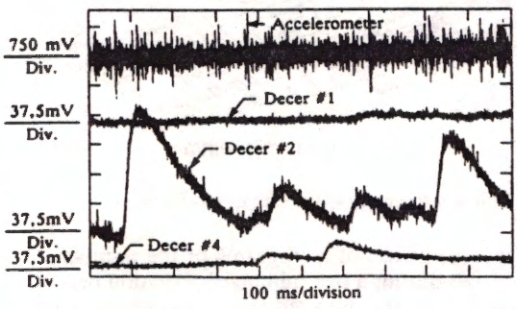

Fig. 9 Acceleration and Decer signal vs time.

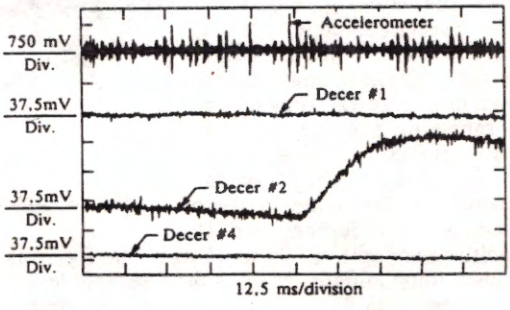

Fig. 10 Time expansion of figure 10.

H3

To better illustrate this statement Figure 10 shows a 125ms time expansion of Figure 9 centered on the last important erosion spike on DECER sensor #2. The beginning of the erosion is clearly associated with the strong triple periodic burst of acceleration of the structure recorded on the top trace. This response can only be attributed to forces with high frequency content acting on the profile as a result of the imploding cavities. Figure 10 also points out an important feature of this excitation. There is strong evidence that this excitation is periodic. It is quite evident that most of the time the response bursts of acceleration are evenly spaced in time though not absolutely always. That this is the case generally, was confirmed in this experimentation program under those conditions where significant erosion was measured. It appears that under the experimentation conditions in the high speed cavitation tunnel explored in this project the main damaging implosions occur at a rate governed by the Strouhal relation plotted in Figure 11. This graph has on the abscissa axis the ratio of the flow velocity to the observed cavity length and on the ordinate axis, the main modulation component of the amplitude envelope of the measured acceleration in the 15 to 35 kHz frequency band. This envelope was frequency analyzed in the 0-5 kHz frequency band with a 800 line FFT analyzer over 100 160ms time records. The frequency resolution of the analysis is 6.25 Hz. To summarize this section, it can be said that erosion is associated with quasi periodic vortices shed away at the closure region of the main leading edge cavity at a frequency related to the flow velocity and the cavity length by a Strouhal relation.

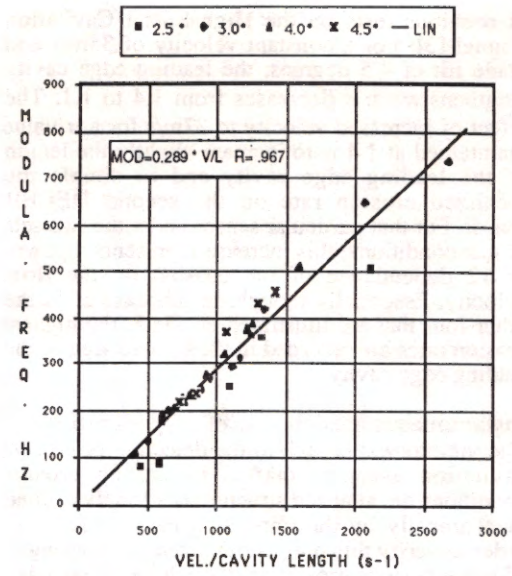

Fig 11 Strouhal relation with modulation of acceleration

Erosion and the acoustic emission sensor

The cavitation impacts hitting the profile at a Strouhal like frequency are also well picked up by the acoustic emission sensor. A set of seven test results recorded with the LOCAN acoustic emission analyzer is shown on Figure 12. They cover the range of average erosion rates from 0.008 to 0.330 mm/a of Titanium. They were measured at the same angle of incidence of 4 degrees and for velocities ranging from 30 to 41 m/s. The figure is a representation of histograms of the number of impulses (hits) initially crossing the threshold level of 54 DB during a one minute observation period. The number with the arrows corresponds to the total number of hits detected in one minute for each test case. As the number of higher amplitude pulses increases, so does the erosion rate. Both the

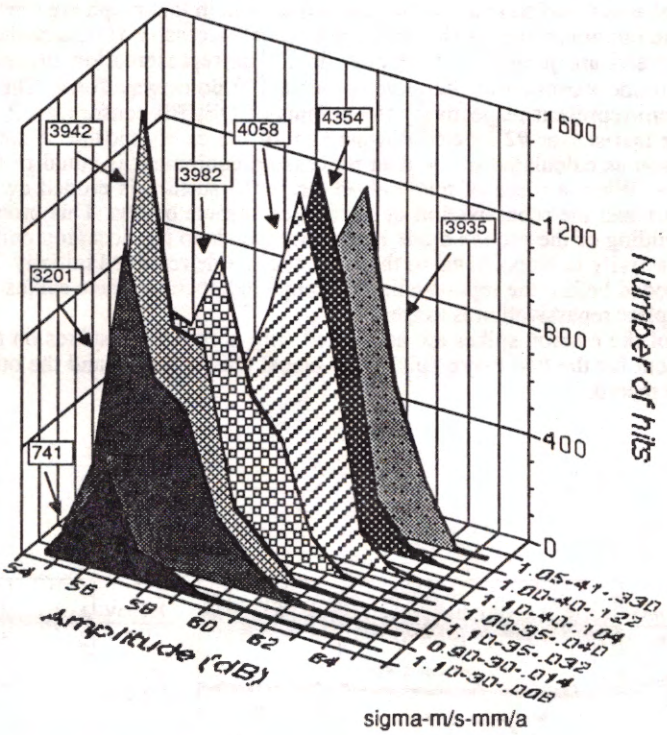

Fig. 12 Acoustic emission spectra at 4° for various erosion rates.

H3

amplitude and the number of impulses appear to influence the erosion rate. Figure 12 is eloquent in this regard; it does not however show the complete picture. The higher amplitude pulses detected for higher erosion also have longer duration above the threshold level and therefore bear even higher energy.

Erosion and acceleration vs velocity.
In the course of data analysis the power laws relating erosion and acceleration to velocity were sought. To do this, at each flow velocity where data was available for the 4 degree incidence angle, the maximum localized erosion rate was plotted against flow velocity. The corresponding MSV of acceleration in the 15-35kHz frequency band was also plotted for the same test conditions. Least squares power law curve fitting was done through the data and the results are shown in Figure 13. Power laws with an exponent of 8.7 for erosion and 5.4 for acceleration were identified. In both cases the correlation coefficient was well above 0.9 indicating a good degree of fit.

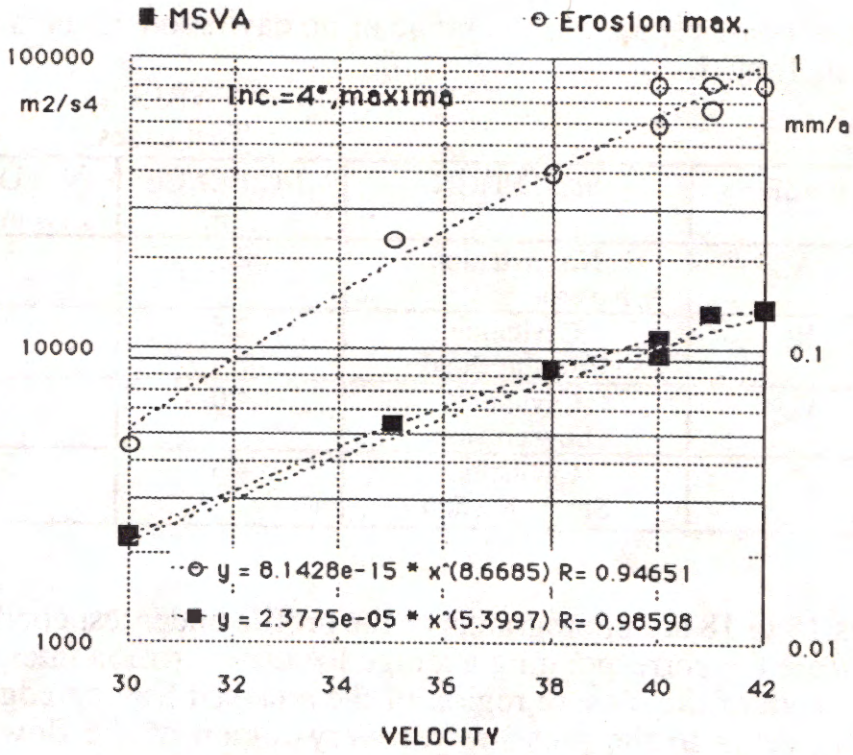

Fig. 13 Power law fit of max. erosion rate and MSVA vs V.

Erosion vs cavity length.
The relation between the erosion rate and the leading edge cavity length was also examined. Figure 14 presents the values measured over all of the explored test conditions. It can be observed that for a given cavity length there is a spread in the corresponding erosion rates for a particular profile design. Factors such as angle of incidence and velocity of the flow as well as the σ value causing the cavity are determinant in its erosive power. There does not appear to exist in our experimentation a unique relation between the cavity length and erosion rate.

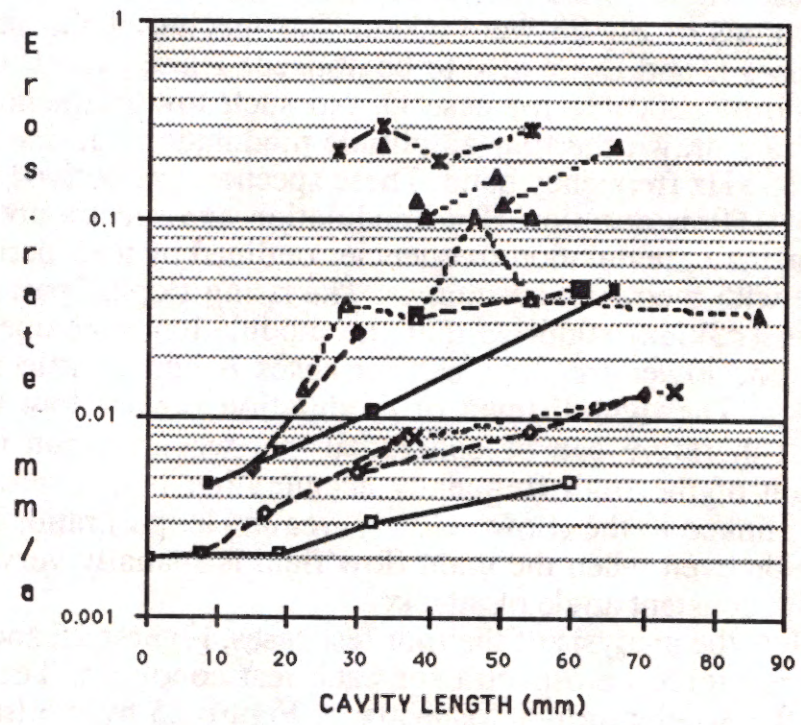

Fig. 14 Average erosion rates vs cavity length.

Erosion vs crest factor.
In the absence of cavitation on the profile, the crest factor (peak to RMS ratio) on the acceleration signal at the accelerometer resonance was 5.0 and remained below 6.0 as long as the cavity length did not exceed 10 mm. Under these conditions, erosion levels on the profile were less than 0.005mm/a, at or just above the detection threshold of the DECER probes. For erosion values of 0.02mm/a and above, the crest factor on the unfiltered accelerometer signal was constantly above 12 varying between 12 and 25. These two observations entrain that high frequency vibration measurements on an operating turbine with a crest factor less than 5 would indicate the absence of an erosion problem on the machine whereas a value of 12 and above would suggest the opposite. This statement remains to be verified on prototypes.

THE SIGNATURE OF EROSIVE CAVITATION.

All of the preceding results have been examined with one objective in mind, the identification of the vibratory characteristics of erosive cavitation vortices. Although many of these characteristics have been outlined as we discussed the various results, we will summarize them by a detailed presentation

of four test cases spanning the range of no cavitation, no erosion, to cavitation with strong erosion, as shown in Table I.

TABLE I
Test cases.

CASE	SITUATION	INCIDENCE deg.	VELOCITY m/s	σ	EROSION mm/a
A	No cavitation No erosion	2.5	35	1.3	0.002
B	Cavitation Eros.threshold	2.5	20	0.81	0.002
C	Cavitation Low erosion	4.0	35	1.1	0.032
D	Cavitation Strong erosion	4.5	35	1.1	0.288

Figures 15 to 18 are photographs of the profile under test conditions A to D respectively. Figures 19 to 23 indicate the corresponding average localized erosion rates. When erosion is present, it occurs at or downstream of the closure region of the attached leading edge cavity. These curves reveal that heavy erosion occurs in the pressure recovery region of the flow behind the cavity where the transient vortices are subjected to collapse due to the steep pressure gradient in the area. Figure 23 shows 4 25 msec excerpts of the unfiltered accelerometer signals sampled at a 10^6 samples/sec rate with a 12 bit resolution A/D converter for the same 4 cases. The vertical axis sensitivity scale is shown at the left of each trace. The appropriate crest factor measured for cases A to D are respectively 5.0, 5.1, 11.3 and 23.8. These values were obtained from the one second time records from which the min/max representations of Fig.23 were taken. The spacing of the strong intermittent acceleration bursts for erosive cases C and D are also to be noticed. These periods correspond to a frequency of 275 Hz for case C and of 200 Hz for case D. No such low frequencies are evident for cases A and B. On Figure 24 are drawn the four amplitude modulation autospectra of the acceleration signal filtered in the 15 to 35 kHz frequency band. These spectra were derived by averaging the autospectra of 100 time records of 160ms duration. The modulation autospectra are presented in the 0-5000 Hz frequency range. The main modulation frequencies outlined by their period in the time record of Fig.23 are easily identified with their first harmonics. The rising sloping part of the continuous spectrum at the lower frequencies(<3kHz) signifies that the modulation envelope is transient in nature with most of its energy at the lower frequencies. For cases A and B little signal energy is contained at the lower frequencies. The overall level of modulation is very low when compared to cases C and D with erosion. It therefore can be concluded that when erosion is present at a measurable level, strong modulation of the high frequency acceleration is also present and is dominated by the Strouhal frequency linked to the (flow velocity)/(cavity length) ratio. This modulation can therefore be present with erosion even when the main flow field is spatially very steady as it is the case in the cavitation tunnel with constant angle of attack.

To complete the analysis of the four test cases, Figures 25 and 26 present respectively the acceleration and inferred force autospectra for each test condition. The inferred force spectra are obtained by dividing the acceleration autospectra of Figure 25 by the transmissibility function of Figure 3. The appearance of cavitation in case B is characterized by a greater level of high frequency content(above 1.5kHz) than in case A even if the flow velocity is significantly lower(20m/s vs 35m/s). The acting forces for their part present spectra with most of the energy concentrated below 3 kHz. For cases A to D, the MSV of the inferred forces in the 62.5 to 3000 Hz frequency band are 233, 61, 30000 and 71324 N^2. It is to be noted that this frequency band corresponds to the one were most of the high frequency acceleration amplitude modulation was observed(see Figure 24) under erosive conditions. If the last value of 71324 N^2 is taken as an example, it would be equivalent in terms of effects to a sinusoidal force with an RMS value of 267 N. With a measured crest factor of about 24 for this case this would lead to a possible instantaneous peak force on the profile over 6000kN. It is not surprising then that erosion occurs under these conditions.

Through the simultaneous measurement of erosion and acceleration analyzed earlier in the section "Instantaneous erosion vs profile acceleration" it was shown that these high level signals are fundamental in the erosion process. Erosive vortices generated at the Strouhal frequency must be linked to the main cavity longitudinal oscillation frequency [1] and this allows to propose the following model for the mean erosive power of the swirling cavities.

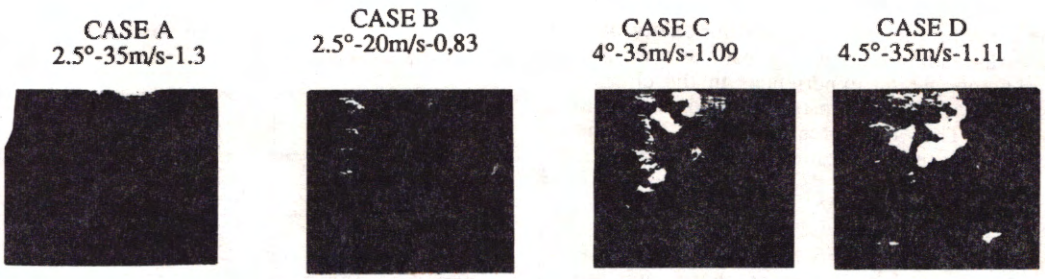

Fig. 15-18 Stroboscopic photos showing cavitation vortices on the profile.

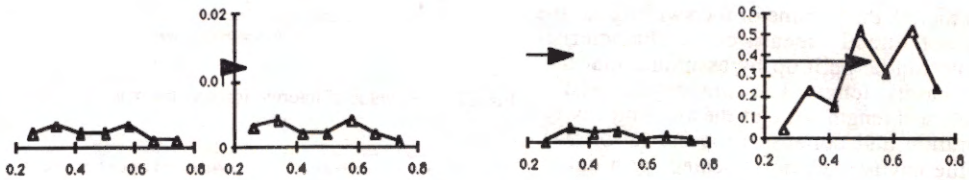

Fig. 19-22. Local erosion rate (mm/a) measured by DECER probes.

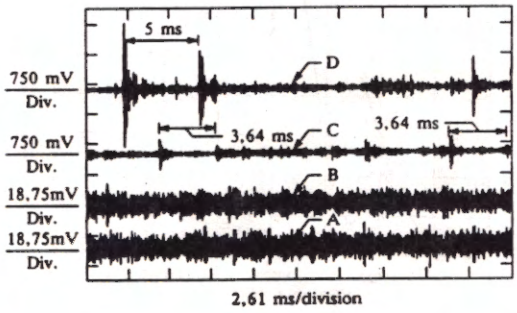

Fig.23 Accelerometer signal vs time.

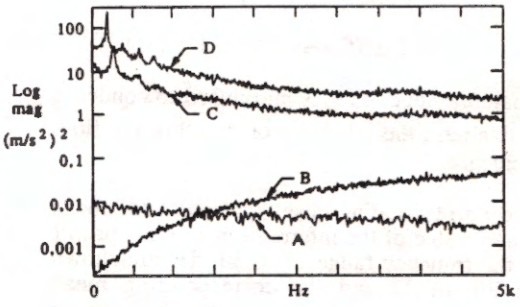

Fig. 24. Amplitude modulation 15-35kHz.

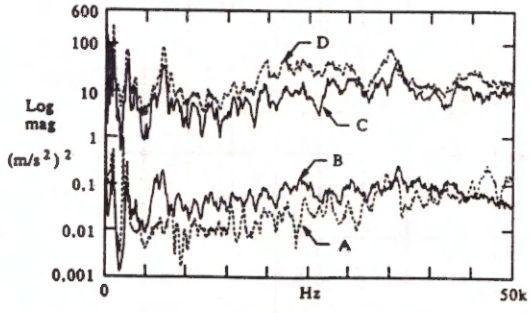

Fig.25. Acceleration autospectra.

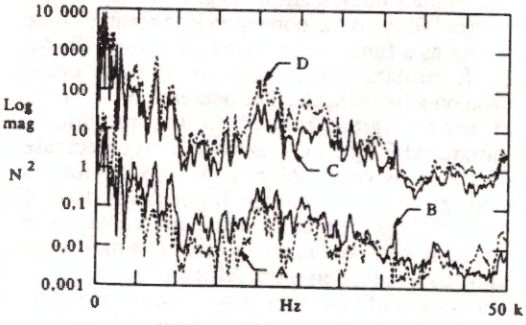

Fig.26. Inferred force autospectra.

H3

The growing process of a swirling cavity over the main leading edge cavity leads to a volume V of vapor which experiences in the closure region a back pressure p_{max} forcing the cavity to collapse. Thus the potential energy E of the cavity collapse can be estimated as follows:

$$E = (p_{max} - p_v)\, V \qquad [J]$$

By introducing the cavity shedding frequency, f, the mean erosive power of these swirling cavities is:

$$\dot{E} = (p_{max} - p_v)\, V\, f \qquad [W]$$

Even though the volume of the swirling cavities V is not directly measured, a characteristic volume can be built up by assuming that the main cavity length l is the characteristic geometrical length scale of the swirling cavity generation and collapse process. It follows that the cavity volume is scaled by a cubic power of l. Moreover the shedding frequency f is driven by a constant Strouhal number law. Thus the mean erosive power can be estimated by the following equation:

$$\dot{E} = 1/2\, \rho F (C p_{max} + \sigma)\, v^3\, l^2 \qquad [W]$$

where the function F is introduced to condense in one term the influence of σ and of the flow incidence.

The corresponding results of the root mean square value of the inferred force on the profile in the frquency range 15 to 30 kHz are shown on Figure 27 and the corresponding mean erosion penetration rate on Figure 28. They are sorted by incidence and sigma values and plotted as a function of the mean erosive power with an F value equal to 1. The linear relationship between these values and the erosive mean power for a given set of incidence and sigma values, leads us to plot the ratio of the inferred force to the corresponding mean erosive power as a function of sigma on Figure 29. All the force data tend to collapse into one curve even on a linear scale. The decrease of this ratio at lower sigma, related to the previously introduced F function, can be seen as a decrease of the erosive efficiency of the cavitation cavities as many cavity implosions do not impact the profile at lower sigma values. The threshold observed in the erosion data makes the same data reduction more difficult.
The review of test cases A to D has shown why and where the erosion takes place. While there is an increase in high frequency content (above 1.5kHz) of the acceleration response of the profile when cavitation starts, the transition to erosive cavitation appears to be gradual and

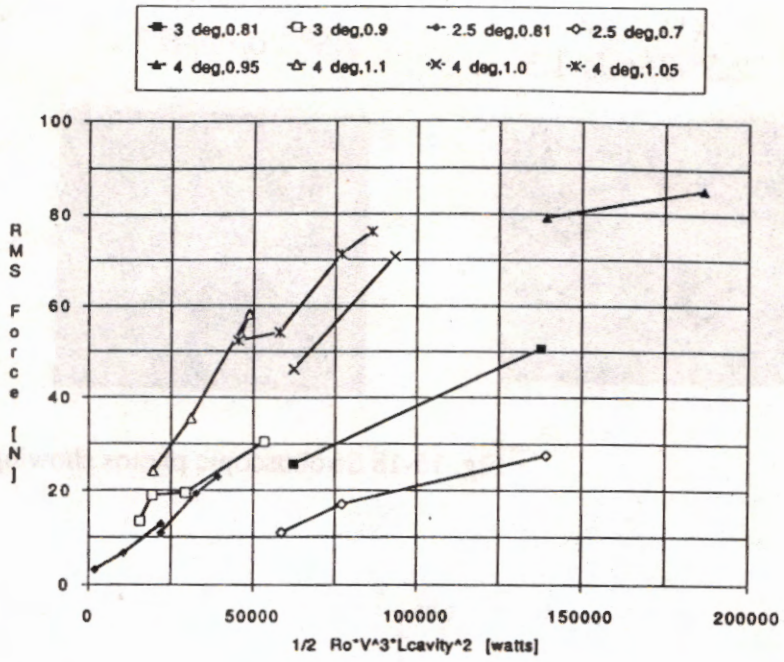

Fig. 27 RMS value of inferred force vs the potential erosive power.

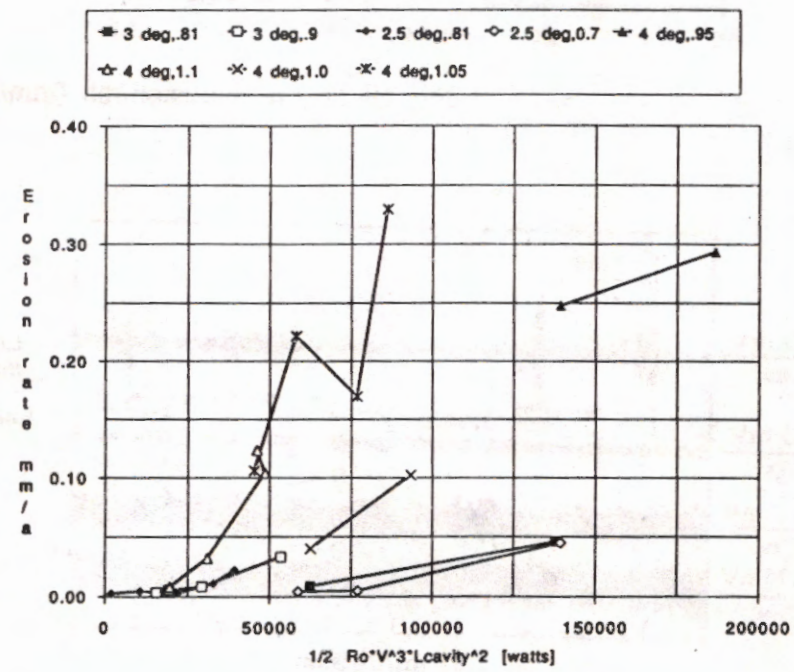

Fig. 28 Average erosion rate vs the potential erosive power.

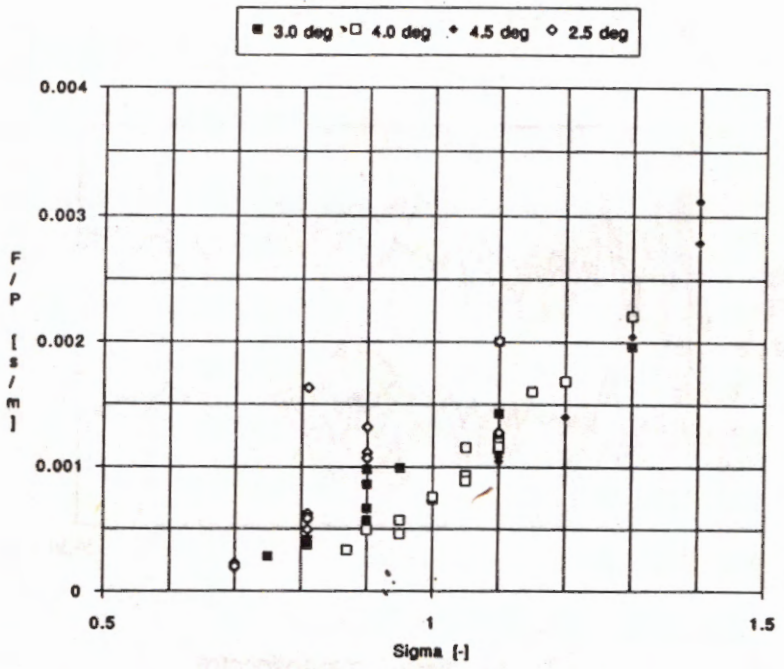

Fig. 29. Force(15-30kHz)-erosive power ratio vs sigma.

H3

amplitude of the stresses imposed on the profile and the resistance of the structure material to this attack. After this transition and for erosion rates larger than 0.01mm/a the following distinctive characteristics of erosive cavitation are observed: a permanent leading edge cavity is present, transient vortices are shed in the closure region of the cavity and implode on the profile mainly at a Strouhal frequency governed by the ratio of the mean flow velocity to the cavity length, rms values of inferred forces acting on the profile are above 100 N while acceleration crest factors of above 12 at high frequencies (90kHz) are measured. With the knowledge of material properties, a measured frequency response function and the calibration data obtained in this experimentation program, it becomes possible to interpret cavitation vibratory data from models or prototypes and establish their erosion potential.

DISCUSSION : APPLICATION OF THESE RESULTS TO MODEL TESTS AND PROTOTYPES.

The linear relationship found between erosion and high frequency acceleration confirm previous results obtained on model and prototype hydroturbines. The high frequency acceleration measure is a practical and simple tool that allows to measure and monitor cavitation erosion in operating hydraulic machines. However its absolute calibration is not universal and must be done for every set-up or design. The use of direct electrochemical detection is difficult and not always possible especially on large machines. The use of transmissibility function is one possible solution.
The well defined Strouhal relation of the acceleration observed at higher erosion and sigma values on the NACA profile is a distinctive characteristic of erosive cavitation. However such a relation will be more difficult to observed on a rotating turbine since the incidence angle can vary during one rotation. For conditions with well defined cavity length the same Strouhal relation should be observable.
On prototypes the historical damage patterns should help in defining the frequency ranges where the effect of erosive vortices should be looked for and possibly related to the cavities observed on models.

CONCLUSION.

The experimental work reported in this paper was oriented towards the identification of the vibratory characteristics of erosive cavitation vortices downstream of a fixed leading edge cavity. The main findings are as follows. A linear relation was found between the mean square value of high frequency acceleration of the profile in the 15 to 35 kHz frequency band and the erosion rate. Erosion was found to be greatest in the closure region of the cavity. This erosion is associated with strong mechanical excitation of the profile occurring at a low Strouhal frequency related to cavity length and flow velocity. This excitation frequency becomes less steady at lower σ values. The peak to RMS ratio of the acceleration signal increases markedly for erosive cavitation. Both the number and the amplitude of the strong implosions determine the erosion level. From the inferred force levels, the observed cavitation shocks produce local stresses much larger than the deformation resistance of the metal. A hydrodynamic relationship in V^3L^2has been found to describe the potential erosive power of the swirling cavities. this potential erosive power of the flow is however controlled in practical terms by the blade design and incidence and by the σ conditions. For low sigma values, where the profile was found to be intermittently excited at the Strouhal frequency, much of this potential energy is shed away in the flow with no resulting damage to the profile.With the above set of information, it will now be possible to make measurements on models and prototypes with a much better view of the vibratory parameters affecting the potential erosiveness of a given design.

ACKNOWLEDGMENT.

The authors are particularly grateful to the Canadian Electrical Association, Hydro-Québec and IMHEF-EPFL who co-funded this research effort. These results would not have been possible without the dedicated assistance of Yan Kuhn de Chizelle who operated the test tunnel during the program, Pierre Lavigne who contributed very creatively at the data acquisition and reduction levels, Jacques Larouche who preincubated the DECER sensors and IMHEF-EPFL technicians who designed and machined the NACA profile with the DECER probes.

REFERENCES

[1] Avellan, F., Dupont, Ph., "Cavitation erosion of hydraulic machines: generation and dynamics of erosive cavities." Proc. 14th IARH Symposium , 20-23 June 1988, Trondheim (Norway).

[2] Avellan, F., Dupont, Ph., Ryhming, I.L., 1988, "Generation mechanism and dynamics of cavitation vortices downstream of a fixed leading edge cavity", Proc. of 17th Symposium on Naval Hydrodynamics, The Hague (The Netherlands), August 29- September 2, 1988, Sessions V, pp. 1 - 13.

[3] Simoneau, R., Avellan, F., Kuhn de Chizelle, Y., "On line measurement of cavitation erosion rate on a 2D NACA profile" Proc. of Third International Symposium on Cavitation Noise and Erosion in Fluid System, ASME, December 1989, San Francisco (USA).

[4] Simoneau, R., Désy, N., Grenier, R., "Electrochemical detection of cavitation erosion on a pump-turbine model", Proc. 13th IAHR Symposium, September 1986, Montréal (Canada).

[5] Bourdon, P., Simoneau, R., Désy, N., Do, N., Grenier, R., "Solving a Severe Cavitation Erosion Problem on a 50 MW Francis Turbine.", Proc. 14th IARH Symposium, 20-23 June, 1988, Trondheim (Norway)

[6] Bourdon, P., Simoneau, R., Lavigne, P., "A vibratory approach to the detection of erosive cavitation", Proc. of Third International Symposium on Cavitation Noise and Erosion in Fluid System, ASME, December 1989, San Francisco (USA).

[7] Simoneau, R., Fihey, J.L., Chincholle, L.,"Effet d'Activation Anodique de la Cavitation Érosive", Proc. 11th IARH Symposium , September 1982, Amsterdam (NL)

[8] Chincholle, L.H., "Study of the Instantaneous Erosion of Cavitation, versus Flow, Pressure and Temperature", Journal of Hydraulic Research, Vol. 26, 1988, No. 1, pp. 67-82.

[9] Abbot, P.A., "Cavitation detection measurements on Francis and Kaplan Hydroturbines", Proc. of Third International Symposium on Cavitation Noise and Erosion in Fluid System, ASME, December 1989, San Francisco (USA).